In vitro cytotoxicity evaluation of biomedical nanoparticles and their extracts

Gautom Kumar Das,[1] Peggy P. Y. Chan,[2] Ailing Teo,[1] Joachim Say Chye Loo,[3] James M. Anderson,[4] Timothy Thatt Yang Tan[1]

[1]*School of Chemical and Biomedical Engineering, Nanyang Technological University, 62 Nanyang Drive, Singapore 637459, Singapore*

[2]*Department of Chemical Engineering, Monash University, Clayton, Victoria 3800, Australia*

[3]*School of Materials Science and Engineering, 50 Nanyang Technological University, Nanyang Avenue, Singapore 639798, Singapore*

[4]*Department of Pathology, Case Western Reserve University, Cleveland, Ohio 44106*

Received 13 January 2009; revised 13 March 2009; accepted 13 March 2009
Published online 30 June 2009 in Wiley InterScience (www.interscience.wiley.com). DOI: 10.1002/jbm.a.32533

Abstract: The present study presents a new approach for evaluating *in vitro* cytotoxicity of nanoparticles. The approach is based on American National Standard ISO 10993-5. Hepatoma HepG2 and fibroblast NIH3T3 cell lines were incubated with nanoparticles, and their associated extracts were derived at 70 and 121°C. Nanoparticles proposed as potential biomedical imaging probes were evaluated on the basis of the detection of metabolic activities and cell-morphology changes. In general, nanoparticles incubated directly with cells showed higher cytotoxicity than their associated extracts. CdSe and core-shell CdSe@ZnS quantum dots resulted in low cell viability for both cell lines. The cytotoxicity of the quantum dots was attributed to the Cd ion and the presence of the nanoparticle itself. A statistically significant ($p < 0.05$) decrease in cell viability was found in higher dosage concentrations. Rare earth nanoparticles and their extracts appear to affect NIH3T3 cells only, with cell viability as low as 71.4% ± 4.8%. Magnetic nanoparticles have no observable effects on the cell viabilities for both cell lines. In summary, we found the following: (1) both direct incubation and extracts of nanoparticles are required for complete assessment of nanoparticle cytotoxicity, (2) the rare earth oxide nanoparticles are less cytotoxic than the Cd-based quantum dots, and (3) the extent of cytotoxicity is dependent upon the cell line. © 2009 Wiley Periodicals, Inc. J Biomed Mater Res 93A: 337–346, 2010

Key words: nanoparticles; cytotoxicity; extracts; hepatoma; fibroblasts

INTRODUCTION

The development of nanotechnology has resulted in a wide array of nanomaterials. Many of these nanomaterials have been proposed for biomedical applications and have drawn enormous attention in recent years.[1–3] Assessment of their potential toxicity is a key concern in bioapplications, as exposure to toxic nanomaterials may lead to detrimental consequences. Although the number of nanoparticle types and applications continues to increase, studies to characterize their effects after exposure and to address their potential cytotoxicity are few in comparison.[4–7] Currently, there is no uniform way of assessing nanoparticle cytotoxicity *in vitro*, and developing a standard protocol for nanoparticle toxicity evaluation is an urgent need.

Nanoparticles used in bioimaging and drug delivery are often bioconjugated to target specific cells. Because nanoparticles are engineered to interact with cells, it is important to ensure that they do not have any adverse effects. For example, nanoparticles may accumulate within cells and lead to intracellular changes such as the disruption of organelle integrity or gene alterations.[6] Semiconductor nanocrystal quantum dots (QDs) have shown promise in biological labeling for their robust and bright emission.[8–10] Most of the studies on potential cytotoxicity of QDs revealed that the core metal constituents of QDs are toxic.[11] If the QDs are exposed to conditions promoting degradation, such as an oxidative environment, free metal ions are leached out and released from the core, causing toxicity. One of the strategies to reduce QD toxicity is to protect the core from degradation with surface coating—a layer of ZnS or a

Correspondence to: T. T. Y. Tan; e-mail: tytan@ntu.edu.sg

silica shell. However, the coating might only be a partial solution, as the release of Cd over a prolonged period of time has not been comprehensively studied.[8] Superparamagnetic iron oxide nanoparticles with tailored surface chemistry have been used in numerous applications, as in magnetic resonance imaging contrast enhancement, hyperthermia, drug delivery, cell separation, and so forth.[12] In terms of cytotoxicity, bare iron oxide nanoparticles exert some toxic effects, whereas surface-coated nanoparticles, especially PEG-coated nanoparticles, have been found to be relatively nontoxic.[13] In recent years, rare earth (RE)-doped nanomaterials have gained attention as a potential bioimaging probes. One of the reasons is its up-conversion ability, which provides a nice window for deep-tissue imaging.[14] However, to the best of our knowledge, there are limited studies on the investigation of the cytotoxicity of the RE-doped inorganic nanocrystals.

In this work, we present a new approach of evaluating the toxicity of nanoparticles through *in vitro* cell viability testing. This method is based on the American National Standard ISO 10993-5, which describes test methods to assess *in vitro* cytotoxicity of medical devices through extracts and direct contact of the device. The Alamar Blue™ assay was selected to quantitatively measure the proliferation and cytotoxicity of nanoparticle-treated human cell lines. This is because Alamar Blue™ is nontoxic, and it is less likely to interfere with normal metabolism. In addition, the one-step Alamar Blue assay is simple to use. Alamar Blue™ can be reduced by $FMNH_2$, $FADH_2$, NADH, NADPH, and cytochromes, whereas the most commonly used tetrazolium salt (MTT) assay can be reduced by all these mentioned substances except cytochromes. The innate metabolic activity of cells results in a chemical reduction of Alamar Blue and causes this redox indicator to change from its blue oxidized form to a reduced form red in color.[15] We believe that this new approach could contribute toward the goal of a generalized and systematic evaluation of toxicity of nanomaterials for biomedical application. In this study, we have chosen nanoparticles that have been proposed as bioimaging probes as model samples. These nanoparticles were amine functionalized to render them dispersible in water, as it has been reported that QDs surface functionalized with amine groups were less cytotoxic.[16]

MATERIALS AND METHODS

Materials

Ytterbium (III) chloride hexahydrate (99.99%), erbium (III) chloride hexahydrate (99.9%), tetramethylammonium-hydroxide (25 wt % in methanol), 1-octadecane (tech. 90%), Igepal CO-520 [Polyoxyethylene(5)nonylphenylether], diethylzinc (1.0*M* solution in hexanes), trioctylphosphine oxide (99%), and oleylamine (tech., 70%), were purchased from Aldrich. Yttrium oxide (99.99%), iron (III) chloride hexahydrate (98%), selenium powder (99%), HNO_3 (analytical reagents, 70%), *n*-octadecylphosphonic acid, and oleic acid (tech. 90%) were purchased from Alfa Aesar. From Fluka, we purchased 3-aminopropyltrimethoxysilane (97%), NaOH (reagent grade, 97%, beads), trioctylphosphine (90%), and hexamethyl disilthiane. Cadmium oxide (99%) was purchased from Hayashi Pure Chemicals. Dulbecco's modified Eagle's medium and penicillin were purchased from Biochrom AG. From JRH Biosciences, we purchased l-glutamine. Phosphate-buffered saline (PBS) (1×, containing 144 mg/L KH_2PO_4, 9000 mg/L NaCl, and 795 mg/L $Na_2HPO_4{\cdot}7H_2O$) and fetal bovine serum were purchased from Invitrogen Corporation. Ethanol, hexane, cyclohexane, and chloroform were of analytical reagent grade and were used as received. Unless stated otherwise, reagents were used as received.

Synthesis and functionalization of nanoparticles

Red-emitting CdSe and CdSe@ZnS QD nanocrystals were synthesized using the methods described in the literature.[17,18] Magnetic γ-Fe_2O_3 nanocrystals were synthesized using a method developed by Park et al.[19] RE-doped and codoped Y_2O_3 were prepared by reacting yttrium oxide powder, oleic acid, sodium hydroxide, and RE-salts as described in our previous work.[20] In every case, the as-synthesized nanoparticles were washed extensively 4–5 times with ethanol to obtain clean particles. Amine functionalization of the nanoparticles was conducted according to the process described by Selvan et al.[21]

Sample preparation

Nanoparticle dosages of 0.0625, 0.10, and 0.25 mg/mL, which are typically used in *in vitro* experimentation, were used to prepare extracts at 37, 50, 70, and 121°C. A dosage of 0.25 mg/mL is approximately double of that used by Jaiswal et al.[22] for the labeling of HeLa cells, and roughly 60 times higher than the concentrations used by Wu et al.[23] for targeting Her2 epitopes on breast cancer cells. However, it is four times less than that used by Derfus et al.[11] Three types of nanoparticle sample solutions at the three sample dosages were prepared with the synthesized nanoparticles: (1) direct dispersion in PBS, (2) formation of nanoparticle extract at 70°C for 24 h in PBS, and (3) formation of nanoparticle extract at 121°C for 1 h in PBS. Samples from (1) were used in the direct contact (DC) method, in which the nanoparticles were incubated directly with the cells. Samples from (2) and (3) were extract samples and were prepared according to the American National Standard ISO 10993-5. The Standard proposes four extraction conditions at 37, 50, 70, and 121°C. The higher temperature conditions at 50, 70, and 121°C are accelerated test conditions used to determine what might be expected at longer time periods at a body temperature of 37°C. However, we have only found ions present at 70 and

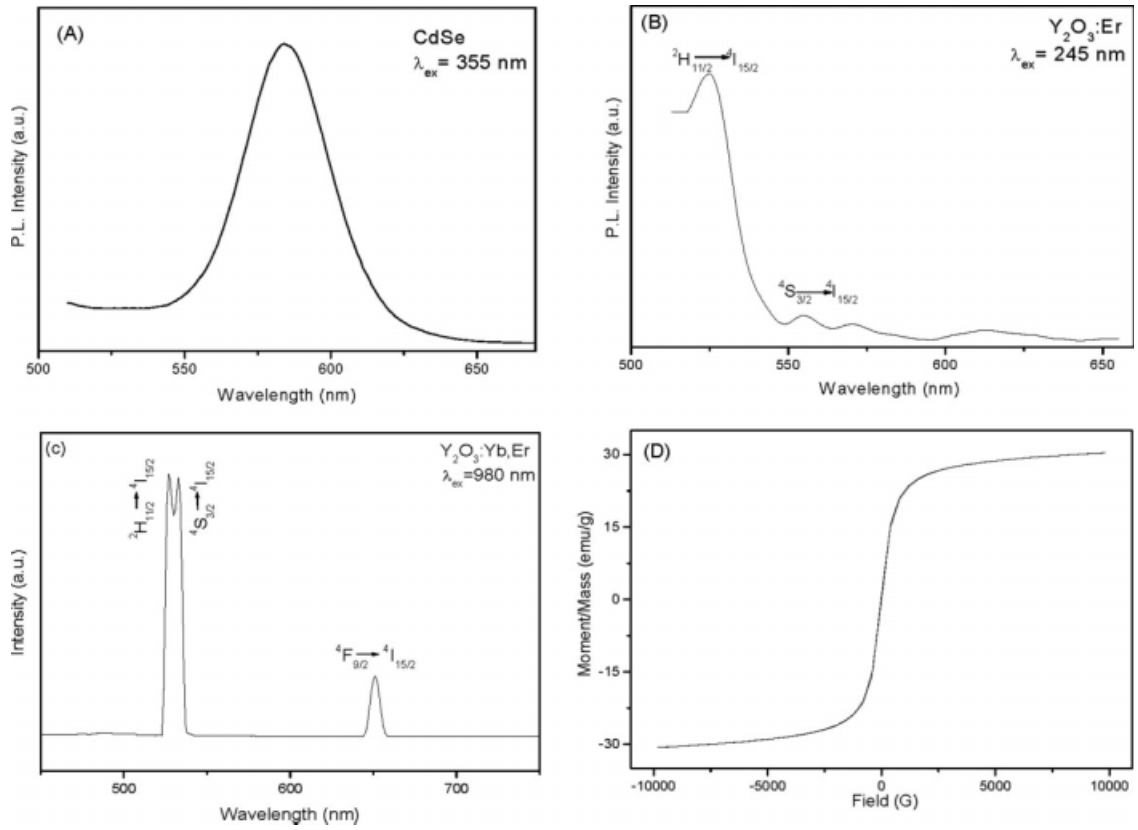

Figure 1. Photoluminescence spectra of (A) CdSe QDs, (B) Y_2O_3: Er, (C) Y_2O_3: Yb:Er, and (D) magnetization curve of γ-Fe_2O_3.

121°C and hence have only reported results based on these extraction conditions. The cells (HepG2 and NIH3T3) were then exposed to the described extracts and nanoparticles for different exposure times (24, 48, and 72 h).

Cell culture and viability

Human hepatocellular liver carcinoma (HepG2), and mouse embryonic fibroblast (NIH3T3) cells were used for cell viability tests. Cells were cultured in Dulbecco's modified Eagle's medium, supplemented with 10% fetal bovine serum, and 1% penicillin/streptomycin at 37°C in a humidified incubator with 5% CO_2. The cells were seeded in 96-well plates, with a concentration of 10,000 cells/well. Twenty-four hours after seeding, spent media was removed and replaced with fresh media. The nanoparticle samples, prepared as described in the earlier paragraph, were then added, followed by incubation for 24, 48, or 72 h. Control experiments of which no nanoparticle samples were added were also prepared for comparison purposes. Cell viability tests were performed using Alamar Blue™ assays (Biosource) to evaluate cell proliferation on the basis of detection of metabolic activities. The tests were repeated three times for each experimental condition to ensure reproducibility.

Characterizations

Transmission electron microscope images were obtained on a JEOL 3010 electron microscope operating on 200 kV. Photoluminescence (PL) spectra were collected on a Shimadzu RF-5301 PC spectrofluorophotometer using a 150 W Xenon lamp as an excitation source. The magnetic properties of these iron oxide nanocrystals were studied using a vibrating sample magnetometer (VSM) (Lake Shore, 7300). Cell morphologies were observed with a Motic AE21 microscope. The concentrations of Cd, Se, Zn, Fe, Yb, and Er ions in the extract solutions were determined using high dispersion induction coupled plasma optical emission spectroscopy ICP-OES (Teledyne Prodigy). For analysis using ICP-OES, 5% nitric acid was added to samples to precipitate the nanoparticles while retaining the free ions in solution for analysis. The samples were centrifuged at 20,000 rpm to remove the nanoparticles, and the solution was further diluted with nitric acid.

In the present study, nanoparticles were characterized to determine their sizes and functionalities. All the nanoparticles used were monodispersed and uniform in size. The size of the CdSe, CdSe@ZnS, and γ-Fe_2O_3 and RE-doped Y_2O_3 nanoparticles were measured to be 6, 7, 8, and 3 $\pm$ 0.2 nm respectively by transmission electron microscope. PL spectra of the CdSe nanocrystals indicated an orange emission band at 585 nm when excited at 355 nm [Fig. 1(A)]. PL spectra of Y_2O_3:Er at 245 nm excitation shows emissions at 525, and 553 nm for $^2H_{11/2} \rightarrow {}^4I_{15/2}$, and $^4S_{3/2} \rightarrow {}^4I_{15/2}$ transition within Er^{3+} ions [Fig. 1(B)]. Figure 1(C) shows the green and red up-conversion spectra of Y_2O_3:Yb:Er at 980 nm excitation. The two peaks in the green emission region centered at 525 and 535 nm correspond to the $^2H_{11/2} \rightarrow {}^4I_{15/2}$, and $^4S_{3/2} \rightarrow {}^4I_{15/2}$

TABLE I
Ion Concentrations of Samples Prepared Under Different Conditions

Nanoparticle Samples	Ion Released	Ion Concentrations (ppm)			
		Cell Medium (Direct Contact Method, 72 h After Incubation)		70°C Extract	121°C Extract
		HepG2	NIH3T3		
CdSe@ZnS	Cd	4.21	5.93	0.51	1.51
	Se	5.34	4.72	NT	3.32
	Zn	4.77	6.20	1.01	1.75
CdSe	Cd	8.41	10.53	2.11	5.11
	Se	9.22	8.87	NT	7.31
γ-Fe_2O_3	Fe	5.23	6.41	1.89	3.15
Y_2O_3:Er	Y	2.46	4.23	2.34	5.24
	Er	0.12	0.65	NT	1.92
Y_2O_3:Yb:Er	Y	2.07	3.78	2.01	3.43
	Er	0.43	NT	NT	1.12
	Yb	NT	NT	NT	0.90

NT, nondetectable (detection limit at 10 ppb).

transitions, respectively, whereas a third peak appearing in the red region at 652 nm corresponds to the $^4F_{9/2} \rightarrow {}^4I_{15/2}$ transition. The magnetization curve of the γ-Fe_2O_3 nanoparticles shown in Figure 1(D) suggests the saturation magnetism of the nanoparticles is 30.5 emu/g.

Statistical analysis

The results are presented as means ± standard deviation. Responses of the cells to the nanoparticles were statistically analyzed using one-way analysis of variance (ANOVA). In all cases, p values lower than 0.05 were considered statistically significant. Significant changes induced by samples are marked by asterisks in the figures.

RESULTS

Nanoparticle extracts

The ion concentration from the cell media was exposed directly to the nanoparticles for 72 h, and the extracts formed at 70 and 121°C is presented in Table I. Extractions at 37 and 50°C for 72 h, which were described in the standard, were also investigated. However, no ions could be detected in the extracts. For CdSe, CdSe@ZnS, and γ-Fe_2O_3 nanoparticles, the highest ion concentration was found when the nanoparticles were exposed directly to the cells

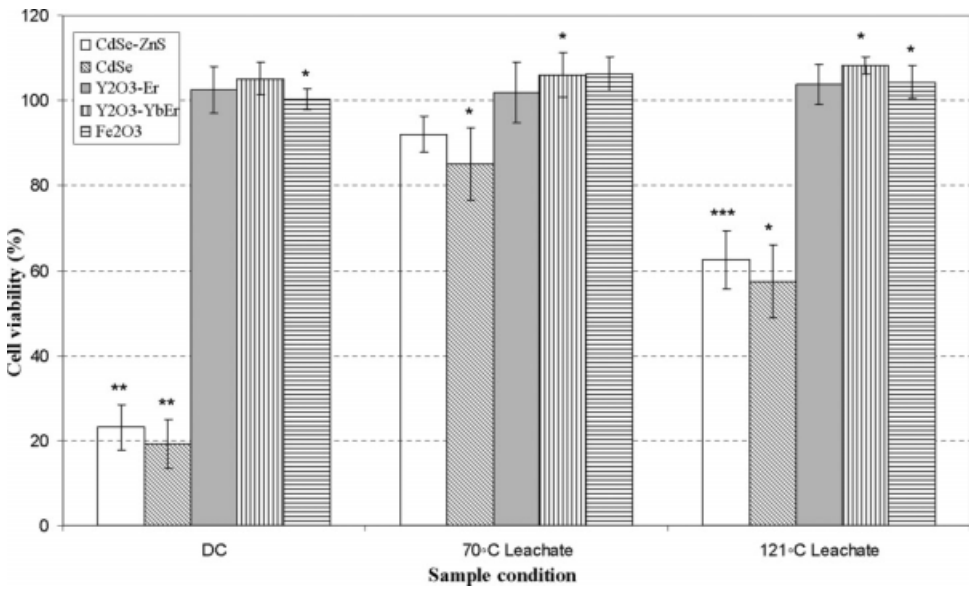

Figure 2. Cell viability of HepG2 cells at 0.25 mg/mL and 72-h exposure. Data are presented as mean ± standard deviation for at least three independent experiments. Value is statistically significant compared to control (ANOVA), *$p < 0.05$; **$p < 0.01$; ***$p < 0.001$.

for 72 h. However, the concentration of RE ions was not significantly higher for the DC method. It is suggested that the harsher conditions at 121°C resulted in more RE ions leaching out when compared with the DC method, in which the incubation took place at 37°C. It is also notable that the amount of ions was generally higher in the NIH3T3 cell media.

In vitro cytotoxicity studies using HepG2 cells

The exposure of the HepG2 cells at a concentration of 0.25 mg/mL with an exposure duration of 72 h is the highest concentration and longest exposure time used in the current study. This condition is referred to as the extreme condition. The HepG2 cells exposed to the extreme condition are shown in Figure 2. Of the five types of nanoparticles, γ-Fe_2O_3, Y_2O_3:Er, and Y_2O_3:Yb:Er studied through the DC method and their associated extracts produced minimal cytotoxicity, with cell viabilities observed to be almost 100%. The results obtained here are consistent with other studies: iron oxide was reported to be of little or no toxicity at low Fe concentration.[12,24,25] Similarly, no significant toxicity was found when the cytotoxicity of Tb-doped Y_2O_3 was studied using HepG2 cells.[20] The results obtained for cell viability were found to be statistically significant with respect to control and are marked by asterisks in Figure 2. CdSe and CdSe@ZnS QDs showed toxicity in the extreme condition with low cell viability, using the DC method and with the 121°C extract. Cells subjected to 70°C extracts have shown comparatively higher cell viability.

The observed changes in cell morphology in Figure 3 are indicative of cytotoxicity. Figure 3(A) shows the confluence of HepG2 control cells. Hepatoma cells generally exhibited spindle-shaped morphology. The morphology of the viable cells was similar to control cells when exposed to relatively nontoxic nanoparticles like Y_2O_3:Er, Y_2O_3:Yb-Er, and γ-Fe_2O_3. However, changes in cell morphology were observed when low cell viability was encountered in the cases of DC method and 121°C extract. For the DC method subjected to CdSe@ZnS QDs, there was evidence of significant cell disruption and ubiquitous cell debris, as shown in Figure 3(B). For cells subjected to 121°C CdSe@ZnS extract, cell membranes showed "blebbling," cell volume reduced, and cells were found to be sparsely packed [Fig. 3(C)].

We have further investigated the effects of higher nanoparticle concentration and longer exposure time using 121°C extracts (Fig. 4). The total amount of Cd ions leached out was dependent on the amount of nanoparticles charged. Our data indicate that with increasing CdSe@ZnS dosage, from 0.0625 to 0.25 mg/mL, the cell viability decreases from 79.5 to

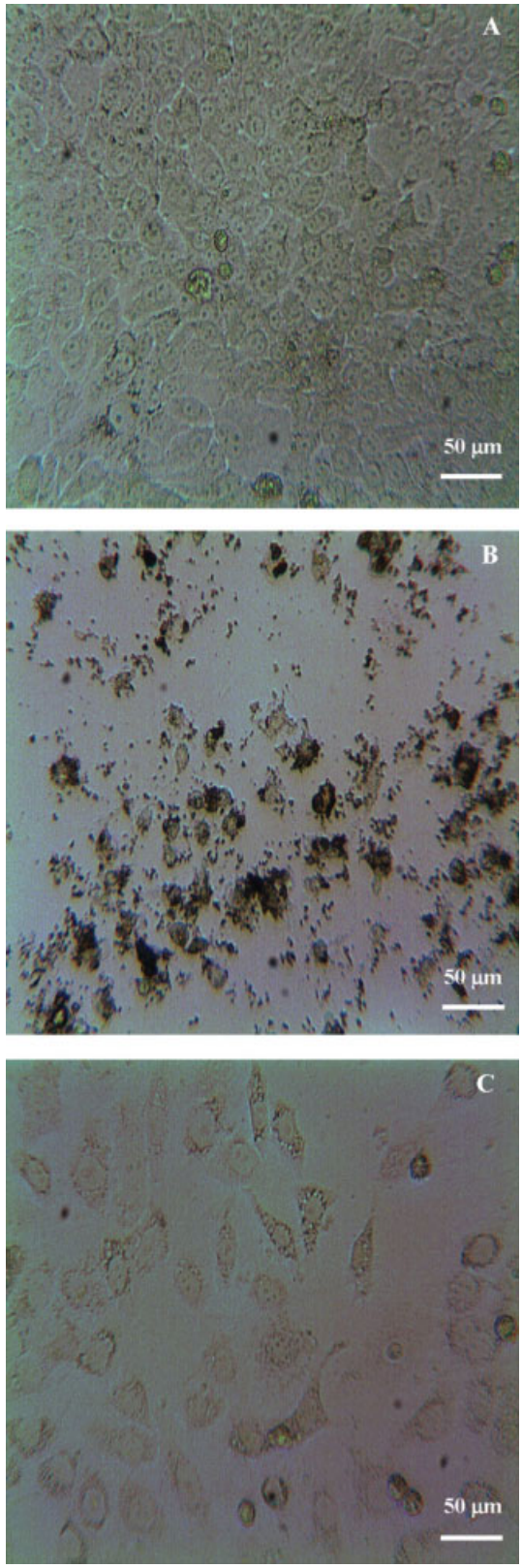

Figure 3. Morphology of HepG2 cells at 0.25 mg/mL and 72-hr exposure observed under microscope: (A) control, (B) cells subjected to DC method with CdSe@ZnS, and (C) cells subjected to 121°C of CdSe@ZnS extract. [Color figure can be viewed in the online issue, which is available at www.interscience.wiley.com.]

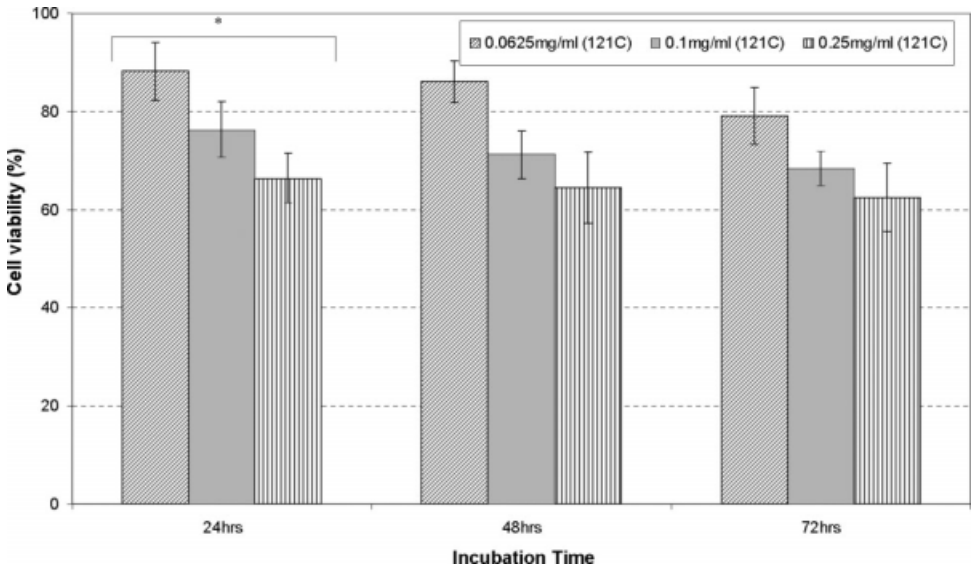

Figure 4. Effects of concentrations and exposure time of CdSe@ZnS nanoparticles on cell viability of HepG2 cells using 121°C extract. Data are presented as mean ± standard deviation for at least three independent experiments. *$p < 0.05$; one-way ANOVA for repeated measures.

61.9%, corresponding to an increase of Cd ion concentration from 0.89 to 1.51 ppm and indicating dose-dependent cytotoxicity. Cell viability did not vary significantly with increasing exposure time.

In vitro cytotoxicity studies using NIH3T3 cells

The cell viability of NIH3T3 cells in response to these nanoparticles and their extracts was investigated (Fig. 5). We started with exposing the NIH3T3 cells to the nanoparticles at the extreme condition. The response of the NIH3T3 cells to the nanoparticles is shown in Figure 5. γ-Fe_2O_3 nanoparticles and associated extracts showed minimal cytotoxicity. NIH3T3 cell viability was found to be depressed in the presence of CdSe and CdSe@ZnS nanoparticles and their extracts, and in fact, the viability was lower compared to that of HepG2 cells. The cell viability was found to be lowest in the DC method, followed by in the extracts obtained at 121°C and then in those obtained at 70°C. Contrary to results from HepG2 cell viability studies, Y_2O_3:Yb:Er and Y_2O_3:Er nanoparticles and their extracts at 70 and 121°C showed lower cell viability. As shown in Figure 5, the cell viability is lowered to 71% when they are

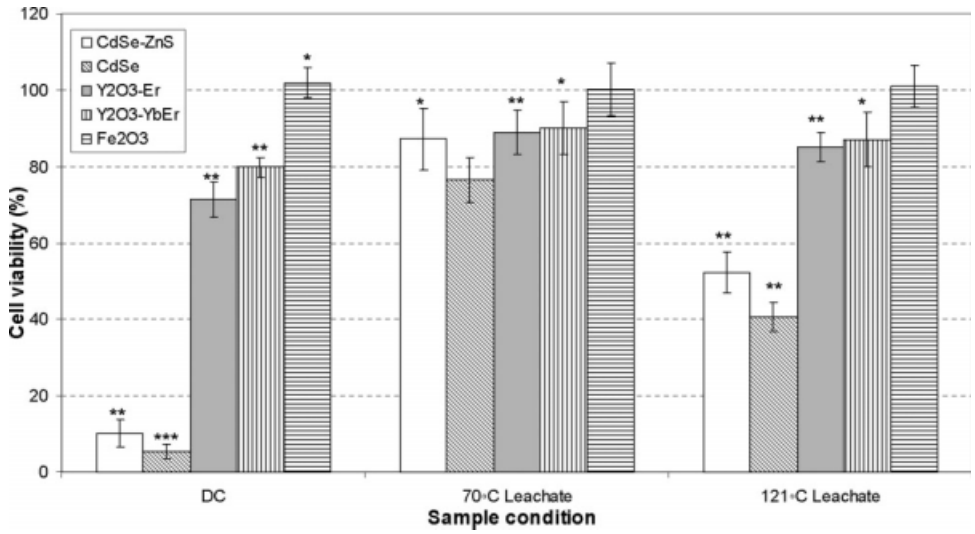

Figure 5. Cell viability of NIH 3T3 cells at 0.25 mg/mL and 72-hr exposure. Data are presented as mean ± standard deviation for at least three independent experiments. Value is statistically significant compared to control (ANOVA), *$p < 0.05$; **$p < 0.01$; ***$p < 0.001$.

incubated with nanoparticles directly, and to approximately 87% for the extracts. Small amounts of RE ions were found in the extracts and cell media (Table I). This finding indicates that NIH3T3 cells were more sensitive to the RE ions than HepG2 cells. The RE ions, though present in a small concentration, caused aggregation and deformation of the NIH3T3 cells [Fig. 6(B)]. When exposed to the 121°C extracts of CdSe@ZnS nanoparticles, the cells were sparsely spaced, and cell debris was observed, indicating a more severe toxicity as compared to the RE oxides [Fig. 6(C)].

Figure 7 shows the effect of dose concentration and exposure time of Y_2O_3:Er nanoparticles with the DC method. We found that the concentration changes in Y ions were minimal (3.98, 3.79, and 4.23 ppm), with increasing exposure time. These results indicate that the presence of the RE nanoparticles is the main contributor to the decrease in cell viability.

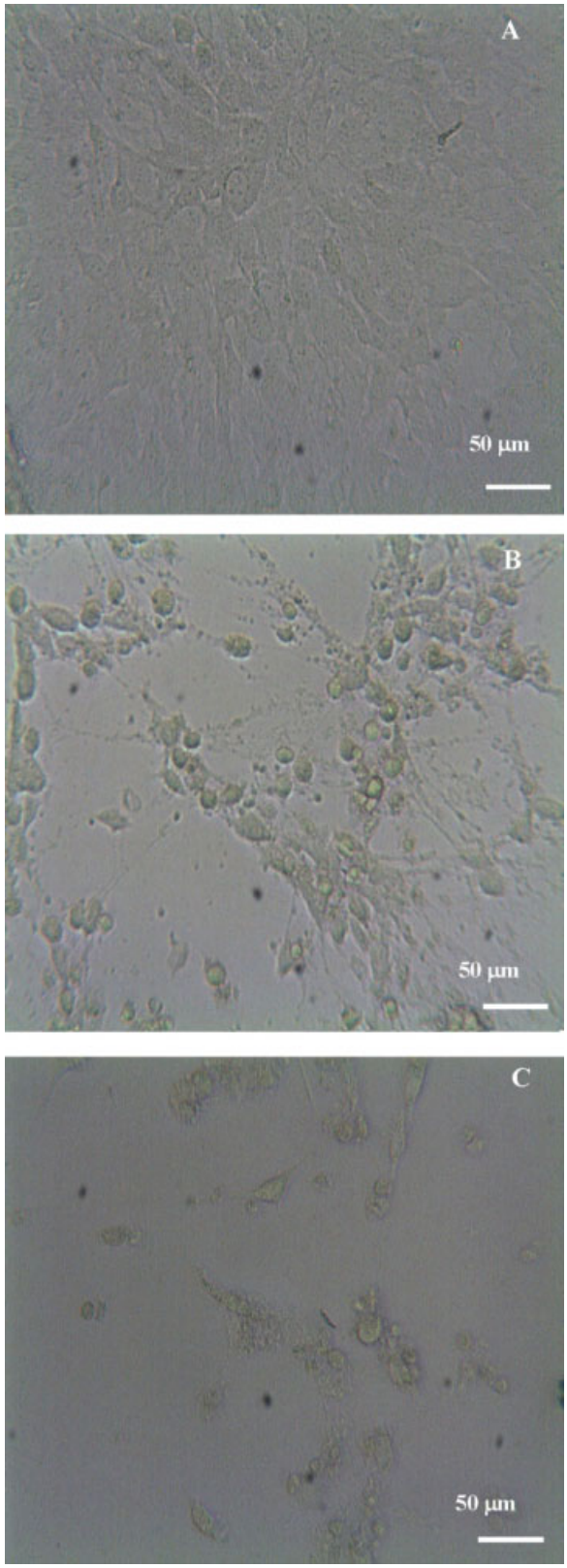

Figure 6. Morphologies of NIH 3T3 cells at 0.25 mg/mL and 72-hr exposure: (A) control, subjected to (B) 121°C extract of Y_2O_3:Er nanoparticles and (C) 121°C extract of CdSe@ZnSe nanoparticles. [Color figure can be viewed in the online issue, which is available at www.interscience.wiley.com.]

DISCUSSION

Effects of nanoparticles and their extracts on cell viabilities

On the basis of the results obtained from the extreme condition, it is apparent that the QDs were toxic under the conditions of the DC method and the 121°C extract. However, as suggested by Figures 2 and 5 and the cell morphology observations, nanoparticles incubated directly with cells (DC method) were more cytotoxic than their respective extracts. The higher cytotoxicity can be attributed to the presence of both the nanoparticle itself and the toxic Cd ions. For HepG2 cells, only the QDs and their associated extracts showed cytotoxic effects. The presence of the other nanoparticles and their ions (Fe, Yb, Y, and Er) produced minimal toxicity to HepG2 cells. However, for NIH3T3 cells, QDs, RE-oxide nanoparticles, and their extracts showed cytotoxicity.

Few mechanisms have been proposed to explain the cytotoxicity of CdSe QDs. Oxidation of QDs can result in the decomposition of CdSe nanocrystals, leading to the release of Cd ions and/or CdSe complex from the core.[26] In addition, QDs can induce reactive oxygen species generation through energy or electron transfer to molecular oxygen.[27] Moreover, the nanoparticles may be internalized by the cells, disrupting the cell membrane and leading to leakage of cellular content, or affecting the functions of cell organelles and nuclei.[6] In our study, high concentrations of Cd and Se ions were found in the cell media after the CdSe and CdSe@ZnS nanoparticles were incubated with the cells for 72 h. The lower cytotoxicity of the CdSe@ZnS is attributed to its ZnS coat-

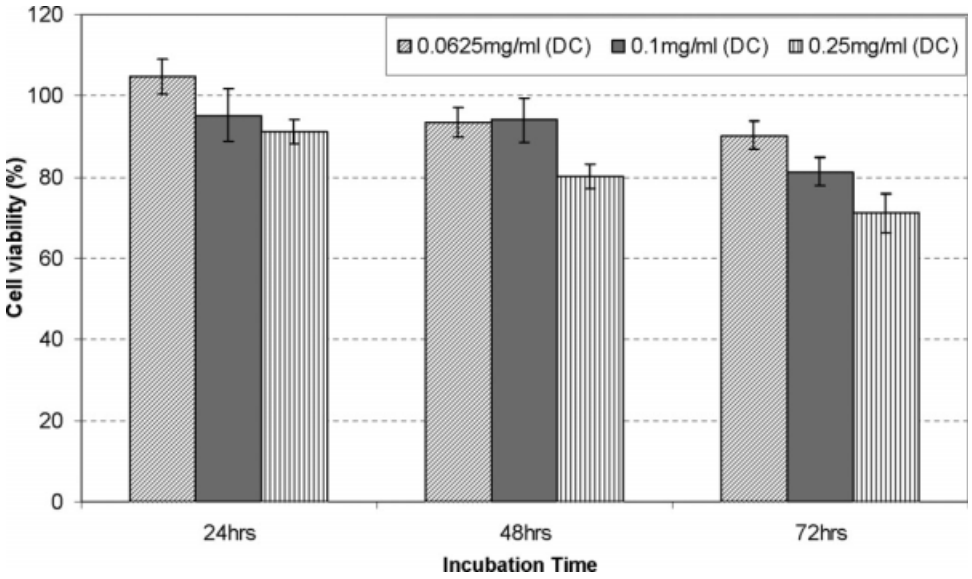

Figure 7. Effects of concentrations and exposure time on cell viability of NIH 3T3 cells using the DC method and Y_2O_3:Er nanoparticles. Data are presented as mean ± standard deviation for at least three independent experiments.

ing, which offers a barrier to the leaching of Cd ions (Table I). The cell viability correlates strongly to the Cd-ion concentrations found in the cell media (via the DC method) and extracts.

Even though RE oxides are temperature resistant,[28] the presence of a small amount of RE ions in the extracts suggests that ions have leached out from the nanoparticle surface, the most probable reason being the high surface area. Very few studies report the toxicity of RE ions at low concentrations. In a study, Hopp et al.[29] tested cytotoxicity of neodymium (Nd) and samarium (Sm) alloy compounds in NIH 3T3 cells and found that the Sm alloy was significantly more toxic than Nd. In an earlier effort, Palmer et al.[30] also tested cerium (Ce), lanthanum (La), and Nd metal cytotoxicity in rat pulmonary alveolar macrophages and reported a low toxicity for these metal ions. Duchen[31] reports that the radii of RE ions are very similar to that of Ca^{2+} (0.099 nm); hence, they may mimic Ca^{2+} ions in the cellular environment. High uptake of calcium causes mitochondrial dysfunction and cell death.

Figures 4 and 7 indicate that higher nanoparticles dosage results in more ions in the media, resulting in lower cell viability. Longer exposure time also depresses cell viability. The presence of the nanoparticles also contributes to higher cytotoxicity. A number of studies have reported similar findings on nanoparticles dose-dependent cytotoxic behavior.[11,32,33] Besides the toxic effects of Cd ions, internalization of the nanoparticles could induce cell death, and the number of nanoparticles internalized correlates to cytotoxicity, as revealed.[34] A higher amount of internalized nanoparticles could induce a greater extent of cell damage or death by disrupting the cell membranes or destroying the cell organelles,[32] as evident in Figure 3(B). In summary, the cell viability of HepG2 is nanoparticle dosage dependent and ion concentration dependent. Toxic ion concentration increases with longer exposure time and higher nanoparticle dosage.

Sensitivity of cells to different nanoparticles

The comparison of the sensitivity of the different cell lines to the CdSe@ZnS and Y_2O_3:Er nanoparticles and their extracts at 121°C is presented in Figure 8. It was found that the cell viability in the DC method was lower than in the extraction method. Both cell lines were sensitive to CdSe@ZnS nanoparticles. However, NIH3T3 cells showed lower

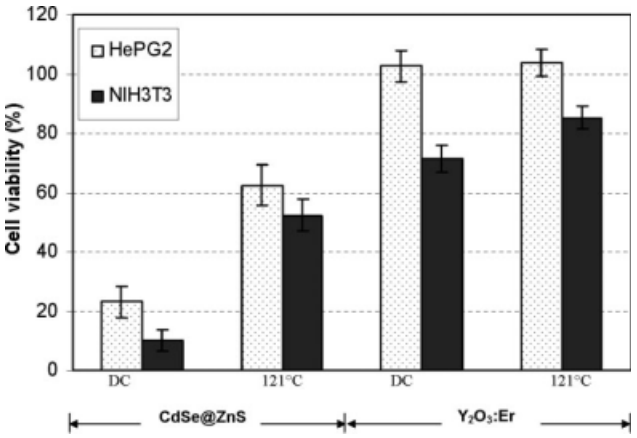

Figure 8. Comparison of HepG2 and NIH3T3 cells sensitivity to different nanoparticles under different experimental conditions. Nanoparticle dosage: 0.25 mg/m.

viability. This indicates that different cell lines respond differently to different nanoparticles. Being a liver cell, HepG2 is capable of the production of metallothionein, a metal sequestering protein, which binds to toxic metal ions to form inert complexes.[35] This could explain the higher tolerance of HepG2 cells toward Cd ion toxicity in all the cases in the current study. We also propose that metallothionein is capable of sequestering RE ions, in particular Y ions. The interaction of metallothionein with metal ions takes place through the thiol groups in the cysteine moieties, which are nucleophiles. Therefore, it is possible that the metallothionein can form complexes with electrophiles such as metal ions. However, studies have shown that the electronic configuration of the metal ions plays a crucial role in forming stable metal complexes.[36] The metal ions may induce the production of metallothionein but may not be able to bind to the protein.[35] Metal ions with a d10 electronic configuration, such as Cd^{2+} and Y^{3+} ions, are suited for complex formation with the multiple cysteine moieties in metallothionein. This could explain why the HepG2 cells were more resilient to the metal ions, manifesting higher cell viability.

CONCLUSION

In this study, we propose a new approach for evaluating the *in vitro* cytotoxicity of nanoparticles by analyses of their extracts obtained at different extraction conditions. This approach contributes to the goal of a generalized and systematic evaluation of toxicity of nanomaterials. From the current study, metal (Cd, Zn, Y, Yb, Er) ions were only found in extracts obtained at 70 and 121°C extraction conditions, as well as in the cell media incubated directly with the nanoparticles. The dosage concentration was found to be a critical factor affecting the cell viability. Cell viability was found to decrease in higher concentrations of Cd ions found in the extracts obtained at 121°C and cell media charged with nanoparticles. In addition, our study has shown that different cell lines have different sensitivity to nanoparticles and metal ion toxicity. In summary, the presence of ions in the extracts suggested that the current proposed method of evaluating cytotoxicity is necessary for nanomaterials intended for biomedical application. Finally, RE-oxide nanoparticles are found to be less cytotoxic than Cd-based QDs and could therefore be suitable candidates for bioimaging probes.

References

1. Ferrari M. Cancer nanotechnology: Opportunities and challenges. Nat Rev Cancer 2005;5:161–171.
2. Burns A, Ow H, Wiesner U. Fluorescent core-shell silica nanoparticles: Towards "Lab on a Particle" architectures for nanobiotechnology. Chem Soc Rev 2006;35:1028–1042.
3. Grainger DW, Castner DG. Nanobiomaterials and nanoanalysis: Opportunities for improving the science to benefit biomedical technologies. Adv Mater 2008;20:867–877.
4. Nel A, Xia T, Madler L, Li N. Toxic potential of materials at the nanolevel. Science 2006;311:622–627.
5. Colvin VL. The potential environmental impact of engineered nanomaterials. Nat Biotechnol 2003;21:1166–1170.
6. Lewinski N, Colvin V, Drezek R. Cytotoxicity of nanoparticles. Small 2008;4:26–49.
7. Gwinn MR, Vallyathan V. Nanoparticles: Health effects—Pros and cons. Environ Health Perspect 2006;114:1818–1825.
8. Alivisatos AP, Gu W, Larabell C. Quantum dots as cellular probes. Annu Rev Biomed Eng 2005;7:55–76.
9. Selvan ST, Tan TT, Ying JY. Robust, non-cytotoxic, silica-coated CdSe quantum dots with efficient photoluminescence. Adv Mater 2005;17:1620–1625.
10. Tan TT, Selvan ST, Zhao L, Gao S, Ying JY. Size control, shape evolution, and silica coating of near-infrared-emitting PbSe quantum dots. Chem Mater 2007;19:3112–3117.
11. Derfus AM, Chan WCW, Bhatia SN. Probing the cytotoxicity of semiconductor quantum dots. Nano Lett 2004;4:11–18.
12. Gupta AK, Gupta M. Synthesis and surface engineering of iron oxide nanoparticles for biomedical applications. Biomaterials 2005;26:3995–4021.
13. Yu WW, Chang E, Sayes CM, Drezek R, Colvin VL. Aqueous dispersion of monodisperse magnetic iron oxide nanocrystals through phase transfer. Nanotechnology 2006;17:4483–4487.
14. Chatterjee DK, Rufaihah AJ, Zhang Y. Upconversion fluorescence imaging of cells and small animals using lanthanide doped nanocrystals. Biomaterials 2008;29:937–943.
15. Henriksson E, Kjellén E, Wahlberg P, Wennerberg J, Kjellström J. Differences in estimates of cisplatin-induced cell kill in vitro between colorimetric and cell count/colony assays. In Vitro Cell Dev Biol Anim 2006;42:320–323.
16. Hoshino A, Fujioka K, Oku T, Suga M, Sasaki YF, Ohta T, Yasuhara M, Suzuki K, Yamamoto K. Physicochemical properties and cellular toxicity of nanocrystal quantum dots depend on their surface modification. Nano Lett 2004;4:2163–2169.
17. Peng ZA, Peng X. Formation of high-quality CdTe, CdSe, and CdS nanocrystals using CdO as precursor. J Am Chem Soc 2001;123:183–184.
18. Wang D, He J, Rosenzweig N, Rosenzweig Z. Superparamagnetic Fe_2O_3 beads-CdSe/ZnS quantum dots core-shell nanocomposite particles for cell separation. Nano Lett 2004;4:409–413.
19. Park J, An K, Hwang Y, Park JG, Noh HJ, Kim JY, Park JH, Hwang NM, Hyeon T. Ultra-large-scale syntheses of monodisperse nanocrystals. Nat Mater 2004;3:891–895.
20. Das GK, Tan TTY. Rare-earth-doped and codoped Y_2O_3 nanomaterials as potential bioimaging probes. J Phys Chem C 2008;112:11211–11217.
21. Selvan ST, Patra PK, Ang CY, Ying JY. Synthesis of silica-coated semiconductor and magnetic quantum dots and their use in the imaging of live cells. Angew Chem Int Ed Engl 2007;46:2448–2452.
22. Jaiswal JK, Mattoussi H, Mauro JM, Simon SM. Long-term multiple color imaging of live cells using quantum dot bioconjugates. Nat Biotechnol 2003;21:47–51.
23. Wu X, Liu H, Liu J, Haley KN, Treadway JA, Larson JP, Ge N, Peale F, Bruchez MP. Immunofluorescent labeling of cancer marker Her2 and other cellular targets with semiconductor quantum dots. Nat Biotechnol 2003;21:41–46.
24. Petri-Fink A, Chastellain M, Juillerat-Jeanneret L, Ferrari A, Hofmann H. Development of functionalized superparamag-

netic iron oxide nanoparticles for interaction with human cancer cells. Biomaterials 2005;26:2685–2694.
25. Wan S, Huang J, Guo M, Zhang H, Cao Y, Yan H, Liu K. Biocompatible superparamagnetic iron oxide nanoparticle dispersions stabilized with poly(ethylene glycol)-oligo(aspartic acid) hybrids. J Biomed Mater Res A 2007;80:946–954.
26. Alivisatos AP. Perspectives on the physical chemistry of semiconductor nanocrystals. J Phys Chem 1996;100:13226–13239.
27. Maysinger D, Lovric J, Eisenberg A, Savic R. Fate of micelles and quantum dots in cells. Eur J Pharm Biopharm 2007;65:270–281.
28. Ramanathan L, Pillis M, Fernandes S. Role of rare earth oxide coatings on oxidation resistance of chromia-forming alloys. J Mater Sci 2008;43:530–535.
29. Hopp M, Rogaschewski S, Groth T. Testing the cytotoxicity of metal alloys used as magnetic prosthetic devices. J Mater Sci Mater Med 2003;14:335–345.
30. Palmer RJ, Butenhoff JL, Stevens JB. Cytotoxicity of the rare earth metals cerium, lanthanum, and neodymium in vitro: Comparisons with cadmium in a pulmonary macrophage primary culture system. Environ Res 1987;43:142–156.
31. Duchen MR. Roles of mitochondria in health and disease. Diabetes 2004;53:S96–S102.
32. Yin H, Too HP, Chow GM. The effects of particle size and surface coating on the cytotoxicity of nickel ferrite. Biomaterials 2005;26:5818–5826.
33. Kirchner C, Liedl T, Kudera S, Pellegrino T, MunozJavier A, Gaub HE, Stolzle S, Fertig N, Parak WJ. Cytotoxicity of colloidal CdSe and CdSe/ZnS nanoparticles. Nano Lett 2005;5:331–338.
34. Chang E, Thekkek N, Yu William W, Colvin Vicki L, Drezek R. Evaluation of quantum dot cytotoxicity based on intracellular uptake. Small 2006;2:1412–1417.
35. Kobayashi K, Shida R, Hasegawa T, Satoh M, Seko Y, Tohyama C, Kuroda J, Shibata N, Imura N, Himeno S. Induction of hepatic metallothionein by trivalent cerium: Role of interleukin 6. Biol Pharm Bull 2005;28:1859–1863.
36. Vašák M. Application of 113Cd NMR to metallothioneins. Biodegradation 1998;9:501–512.